



A simple model of thermal crack pattern formation using the coupled criterion

Un modèle simple de faïençage thermique utilisant le critère couplé

Dominique Leguillon

Institut Jean-Le-Rond-d'Alembert, CNRS UMR 7190, université Pierre-et-Marie-Curie, 4 place Jussieu, 75252 Paris cedex 05, France

ARTICLE INFO

Article history:

Received 20 February 2013

Accepted after revision 8 April 2013

Available online 30 April 2013

Keywords:

Solid mechanics

Fracture mechanics

Thermal cracks

Mots-clés :

Mécanique des solides

Mécanique de la rupture

Fissuration thermique

ABSTRACT

Different mechanisms (cooling, drying, and ageing) lead to the formation of crack patterns on the surface of some materials that are very difficult to describe in detail. We propose a model based on the coupled criterion using two necessary conditions for the nucleation of cracks: an energy condition and a stress condition. This model is applied to a simple example: a plate fixed to a rigid substrate and cooled down on its top face. During slow cooling, it highlights the ability of forming a first lattice of cracks and the subdivision thereof. It also shows that, in a rapid cooling (quenching), the higher the temperature drop, the tighter the cracks network.

© 2013 Académie des sciences. Published by Elsevier Masson SAS. All rights reserved.

R É S U M É

Différents mécanismes (refroidissement, séchage, vieillissement) aboutissent à la formation de réseaux de fissures, appelés faïençage, à la surface de certains matériaux, qu'il est très difficile de décrire dans le détail. Nous proposons ici un modèle qui repose sur l'utilisation du critère couplé faisant appel à deux conditions nécessaires pour la nucléation de fissures : une condition en énergie et une condition en contrainte. Ce modèle est appliqué à un exemple simple : une plaque fixée sur un support rigide et refroidie sur sa face supérieure. Au cours d'un refroidissement lent, il met en évidence la possibilité de formation d'un premier réseau de fissures, puis la subdivision de celui-ci. Il montre également que, lors d'un refroidissement rapide (trempe), plus la chute en température est forte, plus le réseau de fissures est serré.

© 2013 Académie des sciences. Published by Elsevier Masson SAS. All rights reserved.

1. Introduction

Who has not been intrigued, during a walk, by a totally cracked surface of dry mud? Although fundamentally different, several mechanisms give rise to the onset of crack patterns on the surface of materials: the slow or sudden (quenching) cooling of a brittle material such as a ceramic [1], the ageing of a polymer as a result of the action of UV rays [2], the cooling and/or drying of a material initially in a soft state like rock, mud or colloid [3], or even the drying and ageing of pictorial layers of art paintings [4]. In all these situations, we observe extremely complex patterns formed of more or less polygonal cells whose surfaces are not so widely scattered, but still almost impossible to predict in details.

E-mail address: dominique.leguillon@upmc.fr.

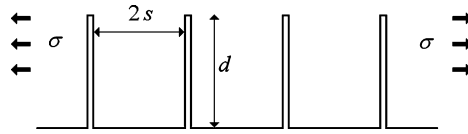


Fig. 1. Parallel edge cracks in a semi-infinite plane submitted to a remote uniform tension.

All these cracks have a common origin: a tensile stress caused by shrinkage due to cooling, a drying or a change in the internal structure of the material. Several authors have tried, using arguments of fracture mechanics, to provide descriptions of the mechanisms that govern this fracturing. Gauthier et al. [3] showed the formation of star-shaped cracks in capillary tubes during evaporation of a solvent from a colloidal solution. Bahr et al. [5] offer a fairly comprehensive analysis of the formation and growth of cracks appearing during a thermal shock on a brittle material, the initial crack spacing is scaled by a coefficient inversely proportional to the square of the temperature drop during the thermal shock. In a similar heat shock experiment, the spacing of cracks and their length correspond, following Jiang et al. [6], to an optimum in a fracture model governed by the Griffith criterion. It is with extensive computing resources that Bourdin et al. [7,8] managed to convincingly simulate the formation of a network of cracks on the surface of a plate subjected to sudden cooling. Their model is based on the variational approach to fracture [9].

Most of works cited above are based on a single condition of energy type, like the Griffith criterion. If the tensile stress that exists in the material plays a mechanical role, typically its contribution to the strain energy, it is never referred to the tensile strength. From our point of view, the crack pattern formation is a nucleation process, and it has been shown that such a mechanism cannot be described by a sole energetic argument; two conditions must be fulfilled simultaneously: one based on energy and involving the material toughness and another based on stress and involving the material strength [10]. We are going to exploit this statement in a very simple framework to describe the nucleation of a crack pattern during a cooling or a drying process in a brittle material. However, unlike the works mentioned above, we are not concerned in the further growth of this network of cracks but only in its onset. It is shown here that if the mechanism is governed by the stress condition, then a sufficient amount of energy can be stored to trigger the nucleation of multiple cracks and fragmentation [11].

Section 2 is a little apart from the core of the paper. Based on known results [12], it is emphasized that the simplifying assumptions used in the sequel make it impossible to determine both the length and spacing of cracks forming a lattice.

Section 3 addresses a first problem of crack pattern formation during the slow cooling (the temperature is assumed to be almost constant throughout the plate thickness) of a plate clamped on its lateral faces. The thermo-elastic solution is analytically known and using the coupled criterion highlights the formation of a rectangular lattice (for simplicity), whose spacing depends on both the toughness and tensile strength of the material. Spacing values are proposed for various materials at the end of the section.

In order to demonstrate the possibility of subdividing the primary lattice, as illustrated in a picture of dry mud, Section 4.1 considers more realistic boundary conditions, analyzing the slow cooling of a plate fixed on a rigid substrate instead of being clamped. The previous solution remains valid in a large part of the plate provided it is thin compared to its length and width. Section 4.2 is devoted to a rapid cooling in the same situation. The temperature profile through the thickness is no longer constant and is approximated by a cosine shape. This simple model allows highlighting the dependence of the lattice spacing on the inverse square of the temperature drop during the rapid cooling (quenching).

The conclusion proposes a discussion on the advantages provided by the use of the coupled criterion in this kind of problem. Then it returns to the difficulty mentioned in Section 2 and emphasizes the need for more comprehensive models and more sophisticated calculations to provide a definitive answer to the problem.

2. Parallel edge cracks in a semi-infinite plane

Before addressing our problem, let us consider a set of parallel edge cracks in a semi-infinite plane submitted to a uniform tension σ . The crack depth and the crack spacing are respectively denoted d and $2s$.

The stress intensity factor K_I at the tip of the cracks depends on these two parameters and there are two limit cases: (i) the cracks are long and close to one another $s \ll d$, (ii) the cracks are short and sparse $s \gg d$ [12]

$$\begin{aligned} \text{(i)} \quad K_I &= \sigma \sqrt{s} F_{12}(d/s) \quad \text{with } F_{12}(d/s) \rightarrow 1 \text{ as } s/d \rightarrow 0 \\ \text{(ii)} \quad K_I &= \sigma \sqrt{d} F_{11}(d/s) \quad \text{with } F_{11}(d/s) \rightarrow 1.122 \times \sqrt{\pi} \text{ as } d/s \rightarrow 0 \end{aligned} \quad (1)$$

The corresponding energy release rate is

$$G = \frac{K_I^2}{E'} \quad \text{with } E' = \frac{E}{1 - \nu^2} \quad (2)$$

where E and ν are respectively Young's modulus and Poisson's ratio of the material. The relation (2) holds under the assumption of plane strain (in plane stress $E' = E$). With l^{tot} equal to the sum of the lengths of all cracks, the change in potential energy δW^p between an initial state without cracks and the final state illustrated in Fig. 1 writes:

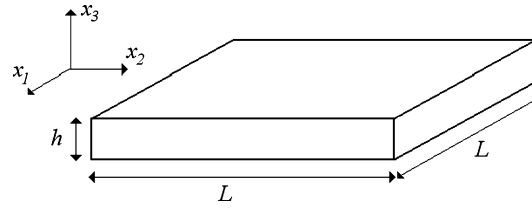


Fig. 2. A plate clamped on all its lateral sides.

$$\delta W^p = I^{\text{tot}} \int_0^d G(\lambda) d\lambda = \begin{cases} I^{\text{tot}} \frac{\sigma^2}{E'} s d & \text{(i)} \\ I^{\text{tot}} \frac{1.122^2 \times \pi}{2} \frac{\sigma^2}{E'} d^2 & \text{(ii)} \end{cases} \quad (3)$$

Note that (i) is an approximation that assumes that formula (1) for long close cracks is valid along most of the integration path.

An energy balance states that failure can occur if this quantity is greater than the energy $G_c I^{\text{tot}} d$ required to create cracks; here G_c is the toughness of the material (fracture energy density) and $I^{\text{tot}} d$ the total created crack surface. Clearly, the first case provides a lower bound for cracks spacing s but no information on cracks depth d , whereas the second one gives a lower bound for cracks depth d , but no information on the crack spacing.

$$\delta W^p \geq G_c I^{\text{tot}} d \Rightarrow \begin{cases} s \geq \frac{E' G_c}{\sigma^2} & \text{(i)} \\ d \geq \frac{E' G_c}{\sigma^2} \frac{1.122^2 \times \pi}{2} & \text{(ii)} \end{cases} \quad (4)$$

In between these two cases, the energy balance provides a relationship between the two characteristic lengths s and d . We will find again this duality in the problem we are now interested in.

3. A plate clamped on all its lateral sides

3.1. The thermo-mechanical model

We consider a thin elastic square plate $L \times L \times h$ ($h \ll L$, Fig. 2) free on the top and bottom faces $x_3 = h$ and $x_3 = 0$ and clamped on all its lateral faces (more precisely, $U_1 = U_2 = 0$, U_3 is not constrained, $\underline{U} = (U_1, U_2, U_3)$ is the displacement field). It is subjected to a slow cooling such that the temperature change $\theta(t) < 0$ is uniform throughout the plate. The thermo-elastic solution is:

$$\begin{cases} \sigma_{33}(t) = 0; & \varepsilon_{33}(t) = \frac{1 + \nu}{1 - \nu} \alpha \theta(t) \\ \sigma_{11}(t) = \sigma_{22}(t) = -\tilde{E} \alpha \theta(t) \\ \varepsilon_{11} = \varepsilon_{22} = 0 \\ \sigma_{12} = \sigma_{23} = \sigma_{31} = 0 \\ \varepsilon_{12} = \varepsilon_{23} = \varepsilon_{31} = 0 \\ \text{with } \tilde{E} = \frac{E}{1 - \nu} \end{cases} \quad (5)$$

Here α is the thermal expansion coefficient of the material, $\underline{\sigma}$ (with components σ_{ij} , $i, j = 1, 3$) the stress tensor and $\underline{\varepsilon}$ (ε_{ij} , $i, j = 1, 3$) the linearized strain tensor.

Following [10], the stress condition for crack nucleation is expressed in terms of the tensile strength σ_c (both σ_c and G_c are assumed independent of the temperature as all material parameters):

$$\tilde{E} \alpha |\theta(t)| \geq \sigma_c \Rightarrow \text{at failure } |\theta(t)| = \theta_c = \frac{\sigma_c}{\tilde{E} \alpha} \quad (6)$$

Fragmentation requires the mechanism to be stress driven [11]; the cooling temperature at failure initiation is fixed by the stress condition. Nothing occurs until $|\theta(t)|$ reaches the critical value θ_c . Thus, depending on the material parameters, a large amount of energy can be stored until the stress condition is reached.

It is reasonably assumed that, if failure occurs, cracks pass entirely through the plate ($d = h$) and that there is no longer any energy stored. Then the change in potential energy δW^p between the initial and final states is:

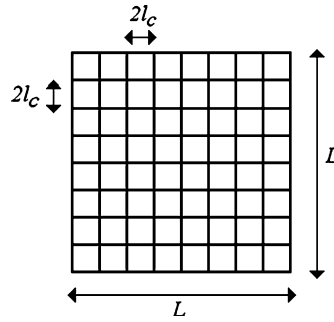


Fig. 3. The rectangular crack pattern.

$$\delta W^P(t) = \frac{1}{2} \int_0^L \int_0^L \int_0^h \underline{\underline{\sigma}} : (\underline{\underline{\varepsilon}} - \underline{\underline{\varepsilon}}^{in}) dx_1 dx_2 dx_3 = \tilde{E} \alpha^2 \theta(t)^2 L^2 h \quad (7)$$

Here $\underline{\underline{\varepsilon}}^{in}$ is the inelastic (thermal) contribution to the total strain $\underline{\underline{\varepsilon}}$. According to (6), the energy balance can be written (l^{tot} already met in Section 2 is the total length of all cracks):

$$\delta W^P(t) \geq G_c l^{tot} h \Rightarrow \frac{l^{tot}}{L} \leq \frac{L}{l_c} = N \quad \text{with } l_c = \frac{\tilde{E} G_c}{\sigma_c^2} \quad (8)$$

At this step, it is almost impossible to describe the crack pattern in its randomness (see Fig. 6 for being convinced); the cells surfaces are not so much scattered but their shape (roughly polygons, often squares or pentagons) is complex. Thus we propose an ultra simplified rectangular array, N is the maximum number of cracks with length L , and the length $s = l_c$ appears to be the theoretical half crack spacing (Fig. 3). In any case, the actual spacing parameter s cannot be smaller than the characteristic length l_c , which can be interpreted as an order of magnitude for spacing in lattices with more complex geometry.

Remark 1. Of course, among other simplifications, it is assumed that the whole lattice (total length l^{tot}) appears almost simultaneously (as reported by authors in some cases [3]). It is important to emphasize that there is no horizontal crack growth, cracks develop in depth.

Remark 2. A noticeable feature is that neither h nor d or α and θ_0 play any longer a role in l^{tot} and l_c . If failure occurs, i.e. if the cooling θ_0 is large enough, then (8) holds true; it is a necessary condition. However, within this model, the exact crack depth d remains unknown like under the assumption (i) in Section 2.

Remark 3. It can be pointed out that the assumption of a thin plate is not necessary in this section. Thus, it can be a model to explain the formation of columns observed in some rock sites, in volcanic rocks such as basalt for instance, provided the assumption that $\theta(t)$ is constant throughout the specimen remains true.

3.2. Some examples of spacing of the primary lattice in various materials

Depending on the material properties, the size of the crack patterns can vary considerably from tens of microns to a few meters.

Ceramics are highly brittle materials subjected to significant cooling during the production process, which is sometimes enough to reveal crack patterns [13].

- Alumina: $E = 350$ GPa, $\nu = 0.3$, $\sigma_c = 300$ MPa, $G_c = 0.04$ MPa mm, $\alpha = 8 \cdot 10^{-6} \text{ K}^{-1} \Rightarrow l_c = 0.22$ mm, crack spacing 0.44 mm, $\theta_c = 75$ K.

The thermal shock resistance of alumina is known to be higher (150 K), but it is determined by quenching (out of the scope of this section) on an unconstrained specimen (out of the scope of this paper, see remark at the end of Section 4.2).

- Polymer: $E = 3.5$ GPa, $\nu = 0.4$, $\sigma_c = 40$ MPa, $G_c = 0.35$ MPa mm, $\alpha = 5 \cdot 10^{-5} \text{ K}^{-1} \Rightarrow l_c = 1.3$ mm, crack spacing 2.6 mm, $\theta_c = 137$ K.

Note that if $\sigma_c = 75$ MPa (for a polymer like PMMA for instance), then the cracks half spacing l_c evolves from 1.3 mm to 0.34 mm.

It is possible also to apply this result to different rocks [14] (although the parameters values are widely scattered in the literature). Unfortunately, it is not possible to find values for α and thus to compute θ_c in the selected examples. It is

noteworthy that the mechanism of pattern formation in sediments like sandstone and limestone is likely due to drying and compaction, not to cooling.

- Sandstone: $E = 16 \text{ GPa}$, $\nu = 0.13$, $\sigma_c = 6 \text{ MPa}$, $G_c = 0.08 \text{ MPa mm} \Rightarrow l_c = 603 \text{ mm}$, crack spacing 1.2 m.
- Limestone: $E = 27.5 \text{ GPa}$, $\nu = 0.23$, $\sigma_c = 3.8 \text{ MPa}$, $G_c = 0.02 \text{ MPa mm} \Rightarrow l_c = 1.7 \text{ m}$, crack spacing 3.4 m.

4. A plate on a rigid substrate

We consider the same plate (Fig. 2) free on the top face $x_3 = h$ and adhering perfectly to a rigid substrate on its bottom face $x_3 = 0$ (i.e. $U_1 = U_2 = U_3 = 0$). It is initially at a given temperature and subjected to a cooling $-\theta_0$ on the top face ($x_3 = h$), no heat exchange is allowed on the bottom ($x_3 = 0$).

For the sake of simplicity, we continue to assume that the lateral faces are clamped and do not allow heat exchange. However, these last conditions are not very realistic; it would be better to suppose that the lateral faces are stress free and at the cooling temperature. In this case, under the assumption of thinness, the thermo-elastic solution is almost the same (biaxial state, see (5) and a vertical heat flux), except in a strip along the edges, whose width is of the same order of magnitude than its thickness h . It can be neglected if h is small enough.

The temperature change through the thickness is denoted $\theta(x_3, t) < 0$ with $\theta(h, t) = -\theta_0$ for any time $t \geq 0$ and $\theta(x_3, 0) = 0$ for any $0 \leq x_3 < h$ and the thermo-elastic solution can still be written (5), replacing the dependence on t only by a dependence on x_3 and t .

The stress condition (6) writes:

$$\tilde{E}\alpha|\theta(x_3, t)| \geq \sigma_c \quad \text{for } h - d \leq x_3 \leq h \quad \Rightarrow \quad |\theta(h - d, t)| = \theta_c \tag{9}$$

since $|\theta(x_3, t)|$ is an increasing function of x_3 for any t . Under the assumption of thinness, it is reasonable again to suppose that $d \simeq h$. If cracks are sufficiently close to one another (see assumption (i) in Section 2), due to the shielding effect, we can assume that the strain energy in the fractured layer (of thickness d) is totally released, then the change in potential energy derives from (7):

$$\begin{cases} \tilde{E}\alpha^2 L^2 \int_{h-d}^h \theta^2(x_3, t) dx_3 \geq G_c l^{\text{tot}} d \quad \Rightarrow \quad \tilde{E}\alpha^2 L^2 \bar{\theta}^2(t) \geq G_c l^{\text{tot}} \\ \text{with } \bar{\theta}^2(t) = \frac{1}{d} \int_{h-d}^h \theta^2(x_3, t) dx_3 \end{cases} \tag{10}$$

4.1. Constant temperature through the plate thickness, subdivision of the primary lattice

If cooling is slow enough, we can suppose that the temperature is constant throughout the plate, then $\theta(x_3, t) = -\theta_0$ and according to (9) and (10):

$$\bar{\theta}^2(t) = \theta_0^2 = \theta_c^2 \tag{11}$$

and the conclusion remains the same.

If cooling is going on, a competition between the in-depth growth of the first network and the formation of a secondary network inside the cells of the first network intervenes now. If d is large and almost equal to h , the tips of the primary network cracks are trapped near the interface with the rigid substrate and the growth is almost inhibited [15]. The second network is likely to occur only if the thickness h of the plate is very small and then small with respect to the cell size $2l_c$ (the lateral faces of the cells are stress free). With $h \ll 2l_c$, the same reasoning can be applied following a new cooling step $-\theta_c$ (the total cooling is now $-2\theta_c$), replacing L by $2l_c$ in (8) leads to:

$$l_2^{\text{tot}} = 4l_c \tag{12}$$

Here l_2^{tot} is the total cracks length of the secondary network within one cell of the primary network. Fig. 4 illustrates this result still under the assumption of a rectangular pattern.

If the process can be iterated (i.e. if $h \ll l_c$), at the next step (total cooling $-3\theta_c$) we get:

$$l_3^{\text{tot}} = l_c \tag{13}$$

leading to many different (rectangular) patterns (Fig. 5).

Fig. 6 shows a crack pattern in mud after drying with visible primary and secondary networks corresponding respectively to wide and narrow opened cracks. The mechanism leading to this crack pattern formation is almost similar, replacing the temperature change by the moisture content change, at least if the mud is no longer in a soft enough state to be considered more or less as an elastic brittle material. However, it is likely that all the material properties (Young's modulus, toughness,

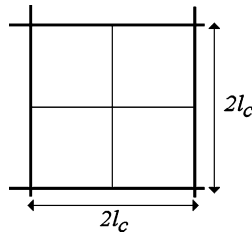


Fig. 4. The subdivision of each cell of the primary network by the secondary network.

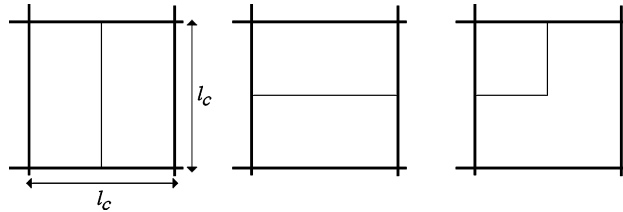


Fig. 5. Different rectangular patterns resulting of the subdivision of each cell of the secondary network.

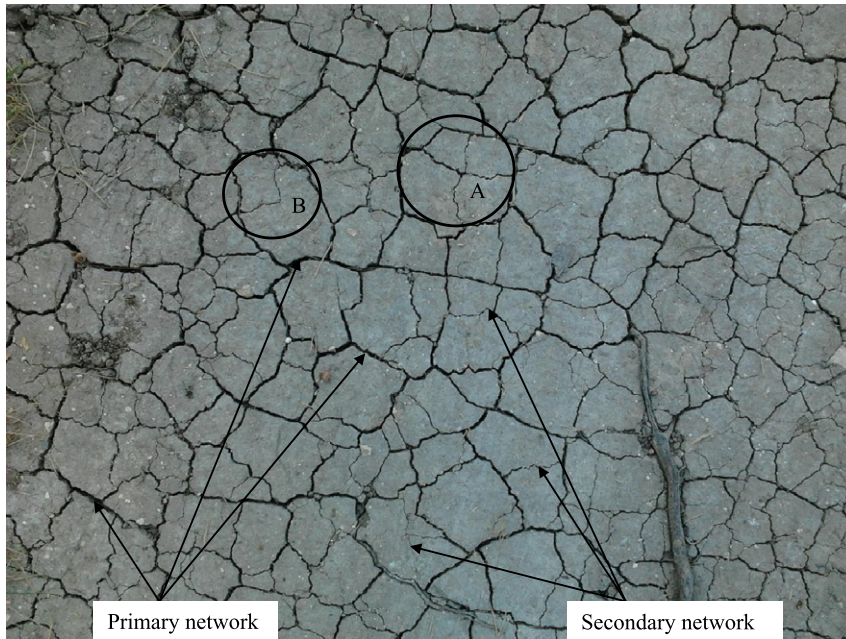


Fig. 6. Formation of a crack pattern in mud after drying, the primary and secondary networks are visible. Among the complex geometries, note the analogy between the subdivision in circle A and Fig. 3 and in circle B and Fig. 4 (right).

strength and even coefficient of expansion) depend on the moisture content and that the model should be improved to be consistent.

Subdivisions are also clearly visible in the polymer after ageing, see Fig. 3(h), p. 1583, of [2].

Of course the scenario proposed in the present work is by far simplified. Sometimes only partially connected networks can be observed [16].

Another explanation for the wide and narrow crack openings could lie in observations of the results exhibited in [1] and [7]. During quenching of a thick specimen, a tight network of cracks appears on the surface. First, the whole set of cracks grows in depth, then at a time an instability occurs and some of the cracks stop while others go on growing. It is likely that cracks belonging to the first family have a narrow opening while the others have a wider one (depending on the crack depth).

However, it must be noted that in the present case cooling is slow and the plate assumed to be thin, while in the other case, cooling is rapid and acting on a thick specimen. The two mechanisms are finally rather different and Fig. 5 seems

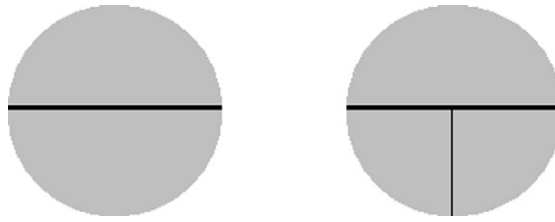


Fig. 7. Primary and secondary networks leading to the formation of a T shaped crack in [3].

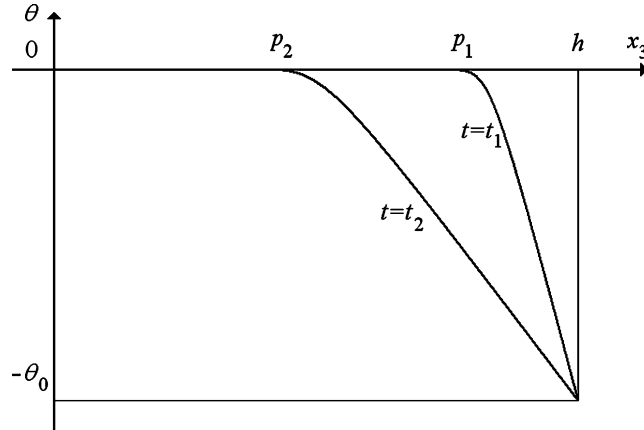


Fig. 8. Temperature change through the plate thickness for different times $t_1 < t_2$. Note that this profile is not affected by the presence or not of straight cracks, but it plays no role in the present analysis.

more favorable to a subdivision mechanism since the supposed secondary network (narrow cracks) has often no continuity from one cell to the neighboring one, whereas the primary one has more.

A similar subdivision was observed in [3] with the formation of T shaped cracks. As described by the authors: “the horizontal bar [...] is formed first and the vertical one later.” (Fig. 7).

4.2. The transient problem, a cosine temperature profile through the plate thickness

The transient solution to the thermal conduction problem with prescribed temperature at one end and vanishing heat flux at the other end of a finite slab is described by series [17]; however, they are not convenient to use, since a large number of terms must be retained to correctly represent the temperature profile, especially in the first steps of cooling. We prefer considering a simplified approximated model which is enough for our purpose. At a given time t , the temperature change through the thickness has the following profile (Fig. 8):

$$\begin{cases} \text{For } 0 < p < h, p < x_3 < h, & \theta(x_3, t) = -\theta_0 \cos\left(\frac{\pi}{2} \frac{h - x_3}{h - p}\right) \\ \text{For } 0 < p < h, 0 < x_3 < p, & \theta(x_3, t) = 0 \end{cases} \tag{14}$$

where the length p is a known function of t . In (14), $h - p(t)$ is similar to the penetration depth of cooling (a length above which cooling is approximately 0, Fig. 8) often approximated by $h - p(t) = \sqrt{4Dt}$ (D is the thermal diffusivity [5,17]), $p = h$ corresponds to the initial condition $\theta(x_3, 0) = 0$, we ignore solutions such that $t > h^2/4D$.

Together with (14), the stress condition (9) leads to a relationship between the time at failure t_c , the crack depth d and the temperature drop $-\theta_0$ on the top surface:

$$\cos\left(\frac{\pi}{2} \frac{d}{h - p(t_c)}\right) = \frac{\theta_c}{\theta_0} \leq 1 \Rightarrow d = \frac{2(h - p(t_c))}{\pi} \cos^{-1}\left(\frac{\theta_c}{\theta_0}\right) \tag{15}$$

Failure occurs only if $\theta_0 > \theta_c$; if $\theta_0 = \theta_c$ then $d = 0$.

Using (14) it comes:

$$\bar{\theta}^2(t) = \frac{\theta_0^2}{2} \left(1 + \frac{\sin(u(t))}{u(t)}\right) \text{ with } u(t) = \frac{\pi d}{h - p(t)} = 2 \cos^{-1}\left(\frac{\theta_c}{\theta_0}\right) \tag{16}$$

Plugging (15) and (16) into (10) leads to:

Table 1The normalized half crack spacing s/l_c for increasing temperature drops $-\theta_0$.

θ_0/θ_c	1.5	2	3	4	5
u	1.68	2.09	2.46	2.64	2.74
s/l_c	0.56	0.35	0.18	0.11	0.07

$$\frac{l^{\text{tot}}}{L} \leq \frac{1 + \frac{\sin(u(t_c))}{u(t_c)} L}{2 \cos^2\left(\frac{u(t_c)}{2}\right) l_c} \Rightarrow s = \left(\frac{\theta_c}{\theta_0}\right)^2 \frac{2 \cos^{-1}\left(\frac{\theta_c}{\theta_0}\right)}{\cos^{-1}\left(\frac{\theta_c}{\theta_0}\right) + \frac{\theta_c}{\theta_0} \sqrt{1 - \left(\frac{\theta_c}{\theta_0}\right)^2}} l_c \quad (17)$$

Results are illustrated in Table 1.

The same trend (Table 1) was observed in [1] in an experiment of quenching of alumina specimens, the crack spacing diminishes as the temperature drop increases. Moreover, a law similar to that proposed by Bahr et al. [5] can be derived from (17): the crack spacing is scaled by a coefficient inversely proportional to the square of the temperature drop θ_0 during the thermal shock.

However, the crack spacing is different (smaller here), but the problem is different as well. In the quenching experiment, the plate is not constrained by a rigid substrate and then can shrink in all directions. Thus the energy released by the cracking mechanism is smaller, resulting in a smaller l^{tot} and thus a larger spacing.

5. Conclusion

The main conclusion to draw is that, during the initial phase of formation of a crack pattern, the scaling length l_c (see (8)) and thus the crack spacing depends strongly on the tensile strength of the material (like $1/\sigma_c^2$). This feature is not present in the analyses cited in Section 1, although the present study tends to prove that it plays a significant role. Indeed, the results in [7,8] are qualitatively impressive and there are few (no?) other works that can lead to such realistic and complex fracture patterns. However, as presented, the approach can definitely not be predictive. The results show more and more complex patterns as a function of an increasing remote load, the I shaped crack is obtained at a given load level, the Y one at a higher level and so on. But during a natural process such as drying or cooling, the second load level cannot be reached without going through the first one, thus the I shaped crack will appear first and then it is impossible to achieve a Y shaped crack pattern (which, in addition, is not an extension of the I crack). One can at best expect a subdivision of the first pattern (as suggested in Section 4.1). The authors of [8] are well aware of the problem and they oppose the static nature of their calculations to a quasi-static evolution of the phenomena. In our opinion, this kind of contradiction exists because the stress condition lacks. The threshold associated with this condition allows inhibition of the formation of some patterns if, for the corresponding load level, the tension in the material is lower than the threshold given by the tensile strength.

The other noticeable point is the size effect associated with parameter L , as already noted in [11] in a different situation, leading also to fragmentation. For a given temperature drop $-\theta_0$, the crack pattern or even its presence or absence rely on this length; clearly, according to (8) and (17), the number of cracks depend on the size of the specimen. The experiments of desiccation of a colloid in [3] are carried out in a capillary tube whose diameter is small (around 1 mm), so it does not likely allow the development of a tight network of cracks, patterns are limited to I, Y and + shaped cracks for the primary network (see the end of Section 4.1).

However, the model presented here has a drawback, i.e. the depth of cracks d at initiation remains undetermined (Section 4) or is a priori prescribed (Section 3). This is due to the assumption that, at the onset, all the energy in the cracked layer is released. It is almost true if cracks are long (and especially close to the plate thickness h) and close to one another, but is clearly wrong for short and sparse cracks.

The improvement of this model and its generalization to other problems (quenching), different geometries and variable material parameters will likely be obtained only through 3D finite element computations providing the profile of the tensile stress and an accurate value of the energy released by fracture. But an additional difficulty rises immediately: crack spacing and depth depend on the ability of the structure to dissipate energy by fracture and both are a priori unknown. This leads [6–8] to treat the problem as an optimization one based on the variational approach to fracture, which consists in searching the crack pattern that minimizes a functional equal to the sum of the strain energy and the surface energy of the created cracks. Could this approach be extended to optimization with constraints? Namely, within the optimization procedure, a crack should be created only if the tensile stress exceeds the tensile strength all along the presupposed new crack path.

References

- [1] Y. Shao, X. Xu, S. Meng, G. Bai, C. Jiang, F. Song, Crack patterns in ceramic plates after quenching, *J. Am. Ceram. Soc.* 93 (2010) 3006–3008.
- [2] G.E. Schoolenberg, A fracture mechanics approach to the effects of UV-degradation on polypropylene, *J. Mater. Sci.* 23 (1988) 1580–1590.
- [3] G. Gauthier, V. Lazarus, L. Pauchard, Shrinkage star-shaped cracks: Explaining the transition from 90 degrees to 120 degrees, *Europhys. Lett.* 89 (2010), <http://dx.doi.org/10.1029/0295-5075/89/26002>.
- [4] L. Pauchard, V. Lazarus, B. Abou, K. Sekimoto, G. Aitken, C. Lahanier, Craquelures dans les couches picturales des peintures d'art, *Reflats de la Physique* 3 (2007) 5–9.
- [5] H.A. Bahr, H.J. Weiss, U. Bahr, M. Hofmann, G. Fischer, S. Lampenscherf, H. Balke, Scaling behaviour of thermal shock crack patterns and tunnelling cracks driven by cooling or drying, *J. Mech. Phys. Solids* 58 (2010) 1411–1421.

- [6] C.P. Jiang, X.F. Wu, J. Li, F. Song, Y.F. Shao, X.H. Xu, P. Yan, A study of the mechanism of formation and numerical simulations of crack patterns in ceramics subjected to thermal shock, *Acta Mater.* 60 (2012) 4540–4550.
- [7] B. Bourdin, C. Maurini, A variational approach to thermal cracks, in: XIIIth ICTAM Conference, Beijing, China, August 19–24, 2012.
- [8] C. Maurini, B. Bourdin, G. Gauthier, V. Lazarus, Crack patterns obtained by unidirectional drying of a colloidal suspension in a capillary tube: experiments and numerical simulations using a two-dimensional variational approach, *Int. J. Fract.* (2013), submitted for publication, <http://dx.doi.org/10.1007/s10704-013-9824-5>.
- [9] G.A. Francfort, J.J. Marigo, Revisiting brittle fracture as an energy minimization problem, *J. Mech. Phys. Solids* 46 (1998) 1319–1342.
- [10] D. Leguillon, Strength or toughness? A criterion for crack onset at a notch, *Eur. J. Mech. A, Solids* 21 (2002) 61–72.
- [11] D. Quesada, D. Leguillon, C. Putot, Multiple failures in or around a stiff inclusion embedded in a soft matrix under a compressive loading, *Eur. J. Mech. A, Solids* 28 (2009) 668–679.
- [12] H. Tada, P.C. Paris, G.R. Irwin, *The Stress Analysis of Cracks Handbook*, third edition, ASME Press, New York, 2000.
- [13] M. Adamovska, L. Gagnepain, P. da Costa, Monolithic catalyst preparation for CNG applications. On the influence of the starting material on the washcoat quality, in: 2nd Int. Symp. on Air Pollution Abatement Catalysis, Cracow, Poland, 8–10 Sept., 2010.
- [14] R.A. Bearman, The use of the point load test for the rapid estimation of mode I fracture toughness, *Int. J. Rock Mech. Min. Sci.* 36 (1999) 257–263.
- [15] D. Leguillon, E. Martin, The strengthening effect caused by an elastic contrast – Part I: The bimaterial case, *Int. J. Fract.* 179 (2013) 157–167.
- [16] V. Lazarus, L. Pauchard, From craquelures to spiral crack patterns: influence of layer thickness on the crack patterns induced by desiccation, *Soft Matter* (2011), <http://dx.doi.org/10.1039/c0sm00900h>.
- [17] H.S. Carslaw, J.G. Jaeger, *Conduction of heat in solids*, second edition, Oxford University Press, Oxford, Great Britain, 1959.